

Dynamics of the magneto-structural phase transition in La(Fe_{0.9}Co_{0.015}Si_{0.085})₁₃ observed by magneto-optic imaging

Original

Dynamics of the magneto-structural phase transition in La(Fe_{0.9}Co_{0.015}Si_{0.085})₁₃ observed by magneto-optic imaging / M., Kuepferling; Bennati, Cecilia; Laviano, Francesco; Ghigo, Gianluca; V., Basso. - In: JOURNAL OF APPLIED PHYSICS. - ISSN 1089-7550. - 115:(2014), p. 17A925. [10.1063/1.4866880]

Availability:

This version is available at: 11583/2525121 since:

Publisher:

AIP American Institute of Physics

Published

DOI:10.1063/1.4866880

Terms of use:

This article is made available under terms and conditions as specified in the corresponding bibliographic description in the repository

Publisher copyright

(Article begins on next page)

Dynamics of the magneto structural phase transition in $\text{La}(\text{Fe}_{0.9}\text{Co}_{0.015}\text{Si}_{0.085})_{13}$ observed by magneto-optical imaging

M. Kuepferling, C. Bennati, F. Laviano, G. Ghigo, and V. Basso

Citation: *Journal of Applied Physics* **115**, 17A925 (2014); doi: 10.1063/1.4866880

View online: <http://dx.doi.org/10.1063/1.4866880>

View Table of Contents: <http://scitation.aip.org/content/aip/journal/jap/115/17?ver=pdfcov>

Published by the [AIP Publishing](#)

Articles you may be interested in

[Contribution of paramagnetic entropy to magnetocaloric effect in \$\text{La}\(\text{Fe}_x\text{Si}_{1-x}\)_{13}\$](#)

J. Appl. Phys. **113**, 17A924 (2013); 10.1063/1.4796191

[Structure evolution and entropy change of temperature and magnetic field induced magneto-structural transition in \$\text{Mn}_{1.1}\text{Fe}_{0.9}\text{P}_{0.76}\text{Ge}_{0.24}\$](#)

J. Appl. Phys. **113**, 043925 (2013); 10.1063/1.4788803

[Reversible solid-state hydrogen-pump driven by magnetostructural transformation in the prototype system \$\text{La}\(\text{Fe},\text{Si}\)_{13}\text{H}_y\$](#)

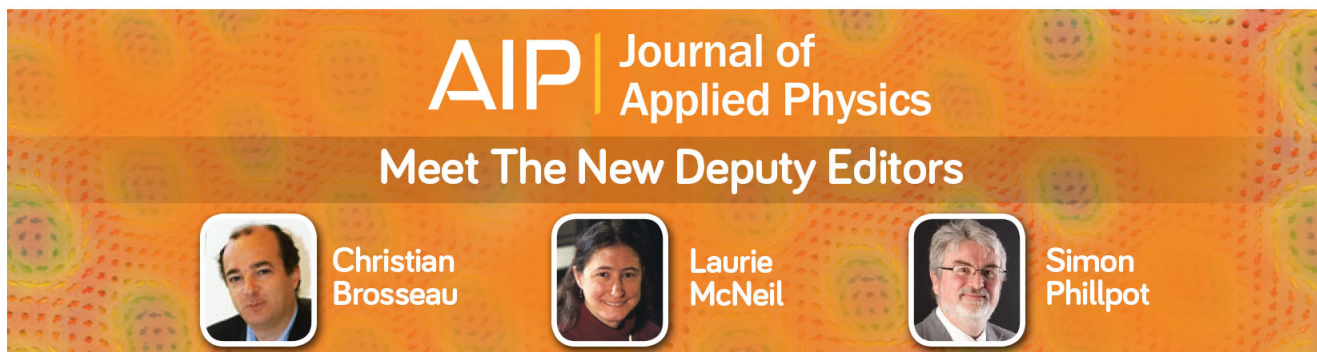
J. Appl. Phys. **112**, 083918 (2012); 10.1063/1.4759438

[Magnetocaloric materials with first-order phase transition: thermal and magnetic hysteresis in \$\text{LaFe}_{11.8}\text{Si}_{1.2}\$ and \$\text{Ni}_{2.21}\text{Mn}_{0.77}\text{Ga}_{1.02}\$ \(invited\)](#)

J. Appl. Phys. **111**, 07A910 (2012); 10.1063/1.3670987


[Structure and magnetocaloric effect in the pseudobinary system \$\text{LaFe}_{11}\text{Si}_2 - \text{LaFe}_{11}\text{Al}_2\$](#)

J. Appl. Phys. **95**, 6924 (2004); 10.1063/1.1667437



AIP | Journal of Applied Physics

Meet The New Deputy Editors

	Christian Brosseau		Laurie McNeil		Simon Phillpot
---	---------------------------	---	----------------------	---	-----------------------

Dynamics of the magneto structural phase transition in $\text{La}(\text{Fe}_{0.9}\text{Co}_{0.015}\text{Si}_{0.085})_{13}$ observed by magneto-optical imaging

M. Kuepferling,^{1,a)} C. Bennati,^{1,2} F. Laviano,² G. Ghigo,² and V. Basso¹

¹*Istituto Nazionale di Ricerca Metrologica (INRIM), Strada delle Cacce 91, 10135 Turin, Italy*

²*Department of Applied Science and Technology, Politecnico di Torino, C.so Duca degli Abruzzi 24, 10129 Turin, Italy*

(Presented 8 November 2013; received 23 September 2013; accepted 22 November 2013; published online 27 February 2014)

We investigate the temperature induced ferromagnetic to paramagnetic phase transition in Co substituted $\text{La}(\text{Fe}_x\text{Co}_y\text{Si}_{1-x-y})_{13}$ with $x=0.9$ and low Co content of $y=0.015$ ($T_c \simeq 200$ K) by means of magneto-optical imaging with indicator film and by calorimetry at very low temperature rates. We were able to visualize the motion of the ferromagnetic (FM)/paramagnetic (PM) front which is forming reproducible patterns independently of the temperature rate. The average velocity of the FM/PM front was calculated to be 10^{-4} m/s during the continuous propagation and 4×10^{-3} m/s during an avalanche. The heat flux was measured at low temperature rates by a differential scanning calorimeter and shows a reproducible sequence of individual and separated avalanches which occurs independently of the rate. We interpret the observed effects as the result of the athermal character of the phase transition. © 2014 AIP Publishing LLC.

[<http://dx.doi.org/10.1063/1.4866880>]

I. INTRODUCTION

Magneto-caloric materials with a magneto-structural phase transition of first order are promising candidates for magnetic refrigeration around room temperature because of the large entropy change at the transition temperature. The first order transition is characterized by hysteresis: both in temperature and magnetic field.¹ This is a strong drawback for application in a refrigeration device, which may be cycled at a frequency of a few Hz. The capacity of a material to perform the transition at these frequencies has been overestimated,² due to the lack of investigations of the transition kinetics.

An example is the alloy $\text{La}(\text{Fe}_x\text{Si}_{1-x})_{13}$ which exhibits a ferro- (FM) to paramagnetic (PM) transition.³ Co substitution rises the transition temperature and lowers the hysteresis.⁴ Previous studies of the kinetics of La-Fe-Si compounds have generated different interpretations. Zhang *et al.* interpreted the observed exponential time dependence of the magnetization as a thermally activated process.⁵ Moore *et al.* described the rate dependence of the magnetic field induced phase transition as an extrinsic effect.⁶ Fujita *et al.* interpreted the kinetics in the framework of the Johnson-Mehl-Avrami (JMA) model.⁷ We observed that most of the kinetics could be attributed to thermal contact effects,⁸ however, our conclusions were merely based on macroscopic observations. As the JMA model is based on the competition between the domain nucleation and the domain propagation at different rates, an investigation of the spatial evolution of the magnetization patterns is needed. Imaging techniques have been applied successfully to phase transitions^{9–11} and magneto-caloric materials in particular,¹² however a time and space characterization is still missing. Here, we present the results of

dynamic magneto-optical observations¹³ and calorimetric measurement on individual transformation avalanches.¹⁴

II. EXPERIMENTAL RESULTS AND DISCUSSION

The temperature induced FM to PM phase transition in polycrystalline Co substituted $\text{La}(\text{Fe}_x\text{Co}_y\text{Si}_{1-x-y})_{13}$ with $x=0.9$ and low Co content of $y=0.015$ ($T_c \simeq 200$ K) was investigated. The sample was prepared by powder metallurgy at Vacuumschmelze GmbH and CoKG.⁴

The magneto-optical imaging (MOI) technique is based on a Kerr microscope, on an optical cryostat and on a magneto-optical indicator film,¹⁵ which consists in a single crystal film of Bismuth-Lutetium substituted iron garnet (BIG), deposited by liquid phase epitaxy on an optical substrate (Gadolinium-Gallium garnet) and equipped with a thin mirror (Ag). The BIG film displays giant Faraday rotation at optical wavelengths and has its spontaneous magnetization in the film plane. When the indicator film is placed in tight contact with a magnetic sample, its magnetization almost freely rotates in presence of stray fields generated by the external source. The light contrast that is measured by the Kerr microscope corresponds to the rotation of the magnetization in the BIG film, which is proportional to the out-of-plane component of the magnetic induction field at the indicator plane. In this way, direct imaging of domains and domain boundaries in ferromagnetic samples can be achieved.¹³

A fragment of $\text{LaFe}_{11.7}\text{Co}_{0.195}\text{Si}_{1.105}$ sample was placed on a Cernox thermometer mounted on top of the cold finger in the cryostat. The indicator film is pressed on the surface of the sample. The temperature rate was remotely controlled (with Labview software) by the liquid helium valve and by the internal heater. The temperature was monitored online, both by the sensor in the cold finger and by the Cernox thermometer. The digital camera was controlled by the same PC,

^{a)}Electronic mail: m.kuepferling@inrim.it.

in order to synchronize the image acquisition with the temperature readings. A uniform, out-of-plane, magnetic field was applied by an electromagnet outside the cryostat. The spatial evolution of the transition is observed by acquiring several image sequences with MOI, during either cooling or heating the sample around the transition temperature, with different temperature rates (10–200 mK/s), and with or without applying a small external field (few mT).

Fig. 1 contains a selection of frames during both cooling and heating experiments, with an applied field of 3 mT. As soon as part of the sample goes through the PM to FM transition, the corresponding sample area is lighting up clearly. There is evidence of a moving FM/PM front whose kinetics follows a precise pattern, which is almost the same in cooling and heating. Different temperature rates in the range 10–200 mK/s were employed and did not significantly alter the observed pattern. The FM/PM phases coexist in a temperature interval of about ~ 5 K, an interval comparable to differential scanning calorimetry (DSC) measurements at similar rates when high thermal contact resistance is present.⁸ This spatial phase separation gives strong support to the first order nature of the observed FM/PM transition. It was observed that this FM/PM front is propagating occasionally in jump-wise fashion, likely correlated with the avalanches detected in calorimetric measurements.⁸ These jumps are position dependent and their spatial pattern is roughly the same, independent of temperature rate and applied field. The speed of the 1D front was estimated by assuming a linear advancement from one image to the next (typical timestamp of 38.6 ms) until a pinning center is reached. The speed of the avalanches is estimated to be of 4×10^{-3} m/s, while the front propagating

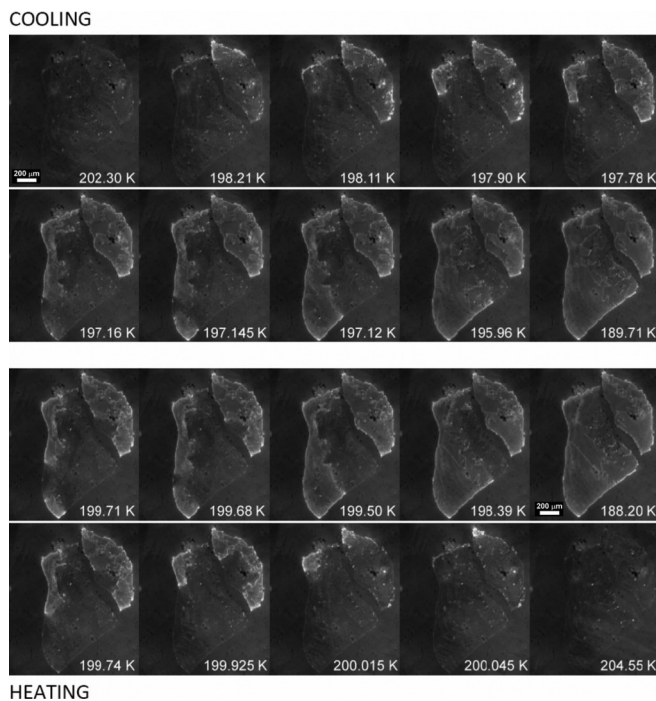


FIG. 1. Selected MOI frames at temperature rates 123 mK/s (cooling: top rows) and 69 mK/s (heating: bottom rows). The first and the last images show the relatively pure PM or FM phase, while the others show phase coexistence. Uniform out-of-plane induction field: 3 mT. The FM phase (brighter parts) displays much larger magnetic flux density than the PM phase (darker parts).

continuously has a speed of the order of 10^{-4} m/s. Careful investigations of the FM/PM front kinetics and its dependence on the external parameters are in progress.

DSC was performed on a second fragment of the same sample down to very low temperature rates in order to disclose the kinetics of individual avalanches. Scans were performed in the range 0.1–200 mK/s. At temperature rates larger than 10 mK/s the avalanches are merged together, while below the individual avalanches start to separate. Comparing the heat flux signals at different rates it appears that the kinetics is dominated by the thermal contact between the sample and the calorimetric cell.⁸ The estimate gives a thermal contact resistance $R \simeq 500$ K/W. Fig. 2 shows the recorded heat flux as a function of the temperature at several rates. The scan was performed from 213.15 K to 193.15 K employing a low rate in the temperature interval 204.15 K–202.15 K. The transition is almost completed (besides small avalanches below the baseline heat flux) within the small interval of ~ 0.53 K. For the time constant of the relaxation of the single avalanches we obtain 5 s independently of the rate. This time constant is related to the thermal contact resistance by $\tau = RC$, where C is the heat capacity of the sample. With an average specific heat of approximately 500 J/kgK and a mass of the sample of 20.54 mg this results in the measured value. Fig. 2, inset, shows how the avalanches randomly change from measurement to measurement. It is worth noting that although the temperature where the avalanche occurs might be slightly different from measurement to measurement, the number of avalanches is always the same, independent of the temperature rate. At higher rates a few smaller avalanches occur in the vicinity of the main ones. From the enthalpy of the single avalanche, the ferromagnetic phase fraction was calculated (see Table I) and compared with the enthalpy of the complete transition (85 mJ) measured at a rate of 4 K/min.

One of the possible interpretations of a rate dependent hysteresis is a thermally activated transition.^{5,7} In thermally activated processes, the energy barrier dividing two local

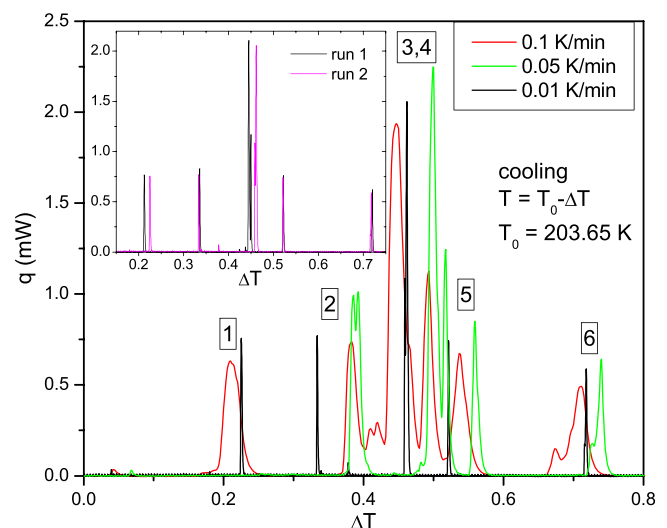


FIG. 2. Heat flux of a $\text{LaFe}_{11.7}\text{Co}_{0.195}\text{Si}_{1.105}$ fragment at low temperature rates around the transition temperature measured by DSC. Inset: Two different scans at 0.01 K/min.

TABLE I. Enthalpy in mJ of single avalanches (as indicated in Fig. 2) at different temperature rates in cooling. FM is the ferromagnetic phase fraction at the rate 0.05 K/min.

Peak	0.1 K/min	0.05 K/min	0.01 K/min	FM
1	9.6	9	9	10.6%
2	7.8	10.6	7.3	12.5%
3	34.1	33.4	8.0	39.3%
4	11	11.8	35.4	13.8%
5	9.4	8.9	8.3	10.5%
6	9.7	8.5	8.3	10.0%
Total	81.6	82.2	76.2	96.7%

minima (in our case the FM and PM phase) is small such that it can be overcome by thermal fluctuations. Thermally activated systems typically show an exponential time dependence. Indeed, by means of *ab initio* calculations small energy barriers were found for the La-Fe-Si compound.¹⁶ Although a statistical analysis of the calorimetric data is still in progress, our preliminary results indicate instead an athermal behaviour. In a certain temperature rate interval, the avalanches appear to be clearly separated and very fast compared to the temperature rate, which means one avalanche occurs at an almost constant temperature. This is confirmed by the high velocity of the FM front during an avalanche. The sequence of avalanches is quite independent of the rate and reproducible. At temperature rates higher than 0.05 K/min the avalanches start to merge together while at slow rates (0.01 K/min) thermal relaxation versus the thermal bath occurs. The athermal character may indicate that large energy barriers are present, which determine the kinetics of the phase transition. Possible causes are defects, stresses due to mismatch of the crystal-structure of the single phases or grain boundaries which act as pinning centers for the propagating FM/PM front, as observed in the magneto-optical measurements. During the temperature cycling, microcracks may occur leading to irreversible aging effects.¹⁷ Therefore, one has to distinguish two levels of phase transition dynamics in La-Fe-Si, the intrinsic one of the defect free crystal which is very fast and might be described successfully by thermal activation and an extrinsic one, presumably due to microstructural defects or thermal relaxation towards a thermal bath. Our results indicate that the latter is relevant for the correct experimental determination of the hysteretic magneto-caloric effect.

III. CONCLUSION

The magneto-optical patterns and the calorimetric measurements of the individual avalanches show that the transformation process is dominated by the pinning of phase boundaries at defects rather than by the nucleation and growth processes. The FM/PM phase nucleates systematically at the same sites and evolve in a rather reproducible fashion. Outside the defective regions the typical domain wall speed is 10^{-4} m/s, while between depinning events it reaches 4×10^{-3} m/s. These jumps are seen also in DSC as isolated avalanches. However, in DSC the rather high speed is masked by the thermal contact resistance. Despite this we note three facts: (i) the avalanche sequence is a rather reproducible process, (ii) we have no evidence of the rate dependence of the nucleation temperatures for the individual avalanches, (iii) the nucleation temperatures have a statistical distribution from run to run. These results indicate an athermal character of the phase transition in which the thermal activation over the energy barriers does not play a relevant role.

ACKNOWLEDGMENTS

The research leading to these results has received funding from the European Community's Seventh Framework Programme FP7/2007-2013 under Grant Agreement No. 310748.

- ¹K. P. Skokov *et al.*, *J. Alloys Compd.* **552**, 310 (2013).
- ²K. Engelbrecht *et al.*, *J. Appl. Phys.* **113**, 173510 (2013).
- ³A. Fujita *et al.*, *J. Appl. Phys.* **85**, 4756 (1999).
- ⁴M. Katter *et al.*, *IEEE Trans. Magn.* **44**, 3044 (2008).
- ⁵H. Zhang *et al.*, *Phys. Rev. B* **70**, 212402 (2004).
- ⁶J. D. Moore *et al.*, *Appl. Phys. Lett.* **95**, 252504 (2009).
- ⁷A. Fujita and H. Yako, *J. Alloys Compd.* **577S**, S48 (2013).
- ⁸M. Kuepferling *et al.*, *EJP Web of Conferences* **40**, 06010 (2013).
- ⁹L. Zhang *et al.*, *Science* **298**, 805 (2002).
- ¹⁰A. Soibel *et al.*, *Nature* **406**, 282 (2000).
- ¹¹M. Manekar *et al.*, *Europhys. Lett.* **80**, 17004 (2007).
- ¹²K. Morrison *et al.*, *Phys. Rev. B* **79**, 134408 (2009).
- ¹³F. Laviano *et al.*, *Physica B* **403**, 293 (2008).
- ¹⁴F. Perez-Reche *et al.*, *Phys. Rev. Lett.* **93**, 195701 (2004).
- ¹⁵L. A. Dorosinskii *et al.*, *Physica C* **203**, 149 (1992).
- ¹⁶M. Kuzmin and M. Richter, *Phys. Rev. B* **76**, 092401 (2007).
- ¹⁷J. Lyubina, *J. Appl. Phys.* **109**, 07A902 (2011).